Journal of Enzyme Inhibition and Medicinal Chemistry, June 2009; 24(3): 646–654

informa
healthcare

Biochemical and structural characterization of TLXI, the *Triticum aestivum* L. thaumatin-like xylanase inhibitor

ELLEN FIERENS[1], KURT GEBRUERS[1], ARNOUT R.D. VOET[2], MARC DE MAEYER[2], CHRISTOPHE M. COURTIN[1], & JAN A. DELCOUR[1]

[1]*Laboratory of Food Chemistry and Biochemistry, Katholieke Universiteit Leuven, Kasteelpark Arenberg 20, Box 2463, 3001 Leuven, Belgium, and* [2]*Laboratory of Biomolecular Modelling and BioMacS, Katholieke Universiteit Leuven, Celestijnenlaan 200G, 3001 Leuven, Belgium*

(*Received 18 February 2008; accepted 21 May 2008*)

Journal of Enzyme Inhibition and Medicinal Chemistry Downloaded from informahealthcare.com by Malmo Hogskola on 12/26/11
For personal use only.

Abstract

Thaumatin-like xylanase inhibitors (TLXI) are recently discovered wheat proteins. They belong to the family of the thaumatin-like proteins and inhibit glycoside hydrolase family 11 endoxylanases commonly used in different cereal based (bio)technological processes. We here report on the biochemical characterisation of TLXI. Its inhibition activity is temperature- and pH-dependent and shows a maximum at approximately 40°C and pH 5.0. The TLXI structure model, generated with the crystal structure of thaumatin as template, shows the occurrence of five disulfide bridges and three β-sheets. Much as in the structures of other short-chain thaumatin-like proteins, no α-helix is present. The circular dichroism spectrum of TLXI confirms the absence of α-helices and the presence of antiparallel β-sheets. All ten cysteine residues in TLXI are involved in disulfide bridges. TLXI is stable for at least 120 min between pH 1–12 and for at least 2 hours at 100°C, making it much more stable than the other two xylanase inhibitors from wheat, i.e. *Triticum aestivum* xylanase inhibitor (TAXI) and xylanase inhibitor protein (XIP). This high stability can probably be ascribed to the high number of disulfide bridges, much as seen for other thaumatin-like proteins.

Keywords: *wheat, xylanase inhibitor, thaumatin-like protein, biochemical characterisation, disulfide bridges, stability, inhibition*

Abbreviations: *TAXI,* Triticum aestivum *xylanase inhibitor; XIP, Xylanase inhibitor protein; TLXI, Thaumatin-like xylanase inhibitor; TLP, Thaumatin-like protein; BSA, bovine serum albumin; IEFTC, Iso-electric focusing titration curve; XTL1, GH11 xylanase from* Trichoderma longibrachiatum *(pI 5.5); XTL2, GH11 xylanase from* Trichoderma longibrachiatum *(pI 9.0); XAN, GH11 xylanase from* Aspergillus niger*; XPF, GH11 xylanase from* Penicillium funiculosum*; XTV, GH11 xylanase from* Trichoderma viride*; XBS, GH11 xylanase from* Bacillus subtilis*; XAO, GH10 xylanase from* Aspergillus oryzae*; EU, enzyme unit; 3D, three dimensional; GH, Glycoside hydrolase family*

Introduction

Endo-1,4-β-D-xylanases (EC 3.2.1.8, further referred to as xylanases) are key enzymes in the degradation of (arabino)xylan, an important constituent of plant cell walls. In *planta*, xylanases are mainly responsible for cell wall remodelling and cell wall degradation upon germination. The best studied xylanases are however of bacterial and fungal origin. While saprophytic micro-organisms use xylanases as part of their toolbox to make nutrients available, pathogenic micro-organisms produce these enzymes to degrade plant cell walls, facilitating the invasion of plant cells [1]. In addition to their role in nature, xylanases are applied in *e.g.* cereal processing and paper and pulp production. They are nowadays often present in bread improvers, as they beneficially affect bread volume and processability of

Correspondence: K. Gebruers, Laboratory of Food Chemistry and Biochemistry, Katholieke Universiteit Leuven, Kasteelpark Arenberg 20, Box 2463, 3001 Leuven, Belgium. Tel: 32(0)16321634. Fax: 32(0)16321997. E-mail: Kurt.Gebruers@biw.kuleuven.be

ISSN 1475-6366 print/ISSN 1475-6374 online © 2009 Informa UK Ltd.
DOI: 10.1080/14756360802321831

RIGHTSLINK

Journal of Enzyme Inhibition and Medicinal Chemistry Downloaded from informahealthcare.com by Malmo Hogskola on 12/26/11
For personal use only.

doughs [2]. They can also be applied in beer production [3], animal feeds [4] and wheat gluten-starch separation processes [5,6]. The majority of the xylanases belong either to glycoside hydrolase family 10 (GH10) or to the structurally unrelated glycoside hydrolase family 11 (GH11) [7].

In 1997, the occurrence of xylanase inhibiting proteins in wheat was discovered. Since then, three types of wheat endogenous xylanase inhibitors have been described, *i.e. Triticum aestivum* xylanase inhibitor (TAXI) [8], xylanase inhibitor protein (XIP) [9], and thaumatin-like xylanase inhibitor (TLXI) [10].

TAXI-type inhibitors are basic proteins (pI $\geq$ 8.0) that occur in two molecular forms, A and B. Form A consists of one single polypeptide chain with a M_r of approximately 40,000, while form B is made up of two peptide chains; one with a M_r of approximately 29,000 is linked to the other with a M_r of approximately 11,000 by one single disulfide bridge ($Cys167_{TAXI}$-$Cys378_{TAXI}$). Form B is derived from form A in *planta*, possibly by the action of specific proteases [8]. TAXI proteins consist of two ß-barrel domains with a few helical segments divided by an extended cleft. They have a close structural relationship with the pepsin-like family of aspartic proteases. They contain six disulfide bridges and are glycosylated to a minor extent [11]. In general, TAXI-type inhibitors are competitive inhibitors of bacterial as well as fungal GH11 xylanases.

Wheat XIP proteins have a M_r of approximately 30,000 and an apparent pI value of 8.8–9.2. These glycosylated proteins have a single elliptical (ß/a)8-scaffold, the top of which is decorated by loops arranged to form a long depression running along one face of the molecule [12]. XIP can inhibit fungal xylanases from both GH10 and GH11 in a competitive manner [13], with some exceptions [14,15]. In addition, the three dimensional structures of XIP in complex with a GH11 xylanase from *Penicillium funiculosum* (XPF), on the one hand, and with a GH10 xylanase from *Aspergillus nidulans*, on the other hand, show a 1:1 complexation ratio for both enzymes and two distinct binding sites. It is hence tempting to hypothesise that complexation with both GH10 and GH11 xylanases can occur at the same time [13,16].

TLXI, the most recently discovered xylanase inhibitor, is a glycosylated thaumatin-like protein with a M_r of approximately 18,000 and a basic pI value ($>$9.3). It is a non-competitive inhibitor which operates by a slow-tight binding inhibition mechanism. TLXI is generally active towards GH11 xylanases with low pH optima. No inhibition activity was observed against a number of GH10 xylanases [10].

Although their direct role remains to be demonstrated, increasing evidence suggests that cereal xylanase inhibitors play a role in the plant's defence mechanism against pathogens [17]. TAXI and/or XIP inhibit GH 11 xylanases of the phytopathogens *Fusarium graminearum* and *Botrytis cinerea* [15,18], and both TAXI and XIP genes are induced by pathogens and wounding [19,20]. In addition, a regulatory role in plant development is disaffirmed by their distinct specificity towards xylanases of microbial origin and their lack of activity against endogenous xylanases [14,21]. Moreover, it was recently demonstrated that xylanase action is indispensable in the infection of plants by the pathogen *B. cinerea* [22].

For TLXI, a 3D structural model was generated based on the crystal structure of thaumatin, using MOE (The Molecular Operating Environment). This model was used on the one hand to support biochemical properties of TLXI (this report) and to determine key residues in the interaction of TLXI with xylanases [23]. Mutational studies of selected surface exposed residues revealed His22 of TLXI to play a critical role in the inhibition of a GH11 xylanase from *Trichoderma longibrachiatum* (XTL1) [23]. The present study provides insight into the TLXI 3D structural features, its stability and optimal working conditions.

Experimental

Materials

All reagents were from Sigma-Aldrich (Bornem, Belgium) and of analytical grade, unless specified otherwise. All electrophoresis and chromatography media and M_r markers were from GE Healthcare (Uppsala, Sweden), unless specified otherwise. Two *T. longibrachiatum* (also known as *T. reesei*) GH11 xylanases [pI 5.5 (XTL1) (NCBI accession number CAA49294) and pI 9.0 (XTL2) (NCBI accession number CAA49293)], *Aspergillus niger* GH11 xylanase (XAN) (NCBI accession number CAA01470), *Trichoderma viride* GH11 xylanase (XTV) (NCBI accession number CAB60757) and Xylazyme-AX tablets were from Megazyme (Bray, Ireland). *P. funiculosum* GH11 xylanase (XPF) (NCBI accession number CAC15487) and GH10 xylanase from *Aspergillus oryzae* (XAO) (NCBI accession number BAA75475) were provided by Dr Nathalie Juge (Institute of Food Research, Norwich, United Kingdom) and by Dr Maija Tenkanen (VTT Biotechnology, Espoo, Finland and University of Helsinki, Finland), respectively. Bovine serum albumin (BSA) and pepsin were from Sigma-Aldrich (Bornem, Belgium). TLXI was purified from wheat whole meal as described by Fierens et al. [10].

Protein content determination

Protein concentrations were determined by the Bradford Coomassie brilliant blue method with BSA as standard [24]. For pure TLXI, protein concentrations were determined spectrophotometrically at 280 nm using a specific absorbance value of 1.457 for 1.0 mg/mL of TLXI (1.0 cm UV-cell path length).

RIGHTSLINK

This value was derived from the amino acid sequence of TLXI [10] using the Protparam tool [25].

Xylanase inhibition assay (Xylazyme-AX method)

Xylanase inhibition activities were determined with the colorimetric Xylazyme-AX method [21]. Xylanase solutions were prepared in sodium acetate buffer (25 mM, pH 5.0) with BSA (0.5 mg/mL) and contained 2.0 enzyme units (EU) per 1.0 mL. 1.0 EU corresponds to an amount of enzyme resulting in an increase in absorbance at 590 nm of 1.0 in the Xylazyme-AX method described below in the absence of inhibitor. Under the conditions of the assay, the xylanase concentrations corresponding to 2.0 EU/mL were 10.2 nM for XAN, 17.8 nM for XTL1, 4.2 nM for XTL2, 23.2 nM for XTV and 4.2 nM for XPF GH11 xylanases and 5.8 nM for XAO GH10 xylanase.

Xylanase inhibitor solutions were diluted in a way assuring a linear response between inhibitor concentration and inhibition activity.

Xylanase solution (0.5 mL) was preincubated for 30 min at room temperature with either inhibitor solution prepared in sodium acetate buffer (25 mM, pH 5.0, 0.5 mL) or the sodium acetate buffer (0.5 mL) (control). The mixture was subsequently kept at 40°C for 10 min. A Xylazyme-AX tablet was then added. After 60 min at 40°C, the reaction was terminated by adding 1.0% (w/v) Tris solution (10.0 mL) and vigorous vortexing. After 10 min at room temperature, the tube was shaken vigorously, the content was filtered through a paper filter and the absorbance was measured colorimetrically at 590 nm against a control, prepared by incubating the Xylazyme-AX tablet with buffer instead of enzyme solution. All measurements were performed in triplicate.

Circular dichroism measurement

The CD spectrum of TLXI was recorded at room temperature with a Jasco J-810 Spectropolarimeter (Jasco Benelux, Maarssen, The Netherlands) using a quartz cell with 0.1 mm path length. Three scans of a TLXI solution [15 μM in sodium acetate buffer (25 mM, pH 5.0)] in the far-UV (200 to 260 nm) were averaged. The ellipticities were expressed as mean residue ellipticities.

Mass spectrometry

The molecular mass of TLXI was analysed by electrospray ionisation mass spectrometry on an Esquire-LC/MS ion trap apparatus (Bruker, Bremen, Germany). TLXI (10 μM, 10 μL) was desalted using a ZipTip C4 (Millipore, Brussels, Belgium), prior to MS analysis.

Stability assessment

Thermal stability. The thermal stability of TLXI was assessed by incubating TLXI solutions at temperatures ranging from 40°C to 80°C for 40 min or by boiling them up to 120 min. After incubation, the inhibitor solutions (0.75 μM in 25 mM sodium acetate buffer, pH 5.0) were cooled on ice and the residual inhibition activities towards XTL1 were measured with the Xylazyme-AX method (*cfr. supra*). All measurements were performed in triplicate and compared to those of a control incubated at room temperature.

pH stability. The pH stability of TLXI was determined by incubating TLXI under different pH conditions for 2 h, followed by adjusting the pH to 5.0 and measurement of the residual inhibition activity. To this end, TLXI (0.3 nmol) was incubated for 2.0 h at room temperature in KCl/HCl solutions (20 mM, pH 1.0 and 2.0, 300 μL), universal buffers (pH 3.0 to 12.0, 300 μL) and KCl/NaOH solutions (20 mM, pH 13.0, 300 μL). Subsequently, the samples were brought to pH 5.0 by adding sodium acetate buffer (250 mM, pH 5.0, 1.7 mL) and the residual xylanase inhibition activities were measured against XTL1 with the Xylazyme-AX method. The universal buffers were prepared as described above. All measurements were performed in triplicate.

Resistance to proteolytic degradation. The resistances of TLXI and BSA (as control) to degradation by pepsin were determined by comparing the SDS-PAGE profiles of both proteins before and after incubation with the protease.

BSA and TLXI (5.5 μM in water, 100 μL) were mixed with pepsin [87 μM in sodium acetate buffer (250 mM, pH 4.0), 45 μL] and incubated at 37°C for 30 min. Control samples were incubated without pepsin. SDS-PAGE was performed on 20% polyacrylamide gels with the Phast System (GE Healthcare), as described in the GE Healthcare separation technique file 110. Sample buffer [125 mM Tris, 4.0% (w/v) SDS, 30% (v/v) glycerol and 0.002% (w/v) bromophenol blue at pH 6.8] was added to each protein sample (1:4 buffer:sample). 2-mercaptoethanol was used as reducing agent [5.0% (v/v)]. After boiling (5 min) and centrifugation (11,000 × g, 3 min), supernatant (4 μL) was loaded onto the gel. The low M_r markers were α-lactalbumin (M_r 14,400), trypsin inhibitor (M_r 20,100), carbonic anhydrase (M_r 30,000), ovalbumin (M_r 43,000), BSA (M_r 67,000) and phosphorylase (M_r 94,000). The gels were silver stained in accordance with the instructions of the manufacturer (GE Healthcare development technique file 210).

Journal of Enzyme Inhibition and Medicinal Chemistry Downloaded from informahealthcare.com by Malmo Hogskola on 12/26/11
For personal use only.

RIGHTSLINK

Determination of cysteine by using Ellmann's reagent

To assay the levels of cysteine and cystine residues in TLXI, analysis with Ellmann's reagent was carried out before and after reduction with sodium borohydride. TLXI (0.64 or 1.28 nmoles) was incubated in the presence of sodium borohydride solution [2.5% (w/v), 45 μL] at 50°C for 60 min. The remaining sodium borohydride was decomposed by addition of HCl solution (20 μL, 1.0 M) and incubation for 30 min at room temperature. As a control, water (65 μL) instead of sodium borohydride and HCl solution (as above) were added to TLXI sample (3.2 nmol).

To 50 μL aliquots of the reduced and non-reduced (control) TLXI samples, Ellmann's reagent [200 μL, 0.05% (w/v) 5,5′-dithiobis(5-nitrobenzoic acid) in 220 mM Tris-HCl buffer, pH 8.2] was added. After incubation for 5 min at room temperature, the absorbance at 415 nm was measured. The level of cysteine residues was calculated based on a standard curve constructed with glutathione (0–1200 μM) in water.

Conditions for maximal inhibition activity

Optimal temperatures for inhibition. The optimal temperatures for TLXI inhibition activities against XTL1, XAN, XPF and XTV GH11 xylanases were determined by performing the Xylazyme-AX method at incubation temperatures ranging from 20°C to 60°C. A TLXI solution (0.27 μM) was prepared in sodium acetate buffer (25 mM, pH 5.0) and the enzyme solutions (2.0 EU/mL; EU determined at 40°C) were prepared in the same buffer with BSA (0.5 mg/mL). All measurements were performed in triplicate.

Optimal pH values for inhibition. The optimal pH conditions for TLXI inhibition activity against XTL1, XAN, XPF and XTV GH11 xylanases were determined by performing the Xylazyme-AX method using buffers with varying pH. To this end, TLXI solutions (0.27 μM) were prepared in universal buffers of pH 3.0 to pH 7.0. The xylanase solutions (2.0 EU/mL; EU determined in universal buffer pH 5.0) were prepared in the same buffers with BSA (0.5 mg/mL). The universal buffers were prepared from a stock solution containing 30 mM citric acid, 30 mM KH_2PO_4, 30 mM H_3BO_3 and 20 mM diethyl barbituric acid in deionised water (1.0 L). To portions of this stock solution, HCl (2.0 M) or NaOH (2.0 M) was added to adjust the pH. All measurements were performed in triplicate.

Iso-electric focusing titration curve analysis

IEFTC analysis was performed with the Phast System (GE Healthcare) using polyacrylamide gels containing ampholytes (pH 3.0 to 9.0). First, carrier ampholytes were subjected to an electric field to generate a pH gradient. The gels were then rotated 90° and protein samples were applied perpendicular to the pH gradient using an eight-well applicator. The migration step was then executed. Prior to application on the gels, the samples (200–1200 ng/well of TLXI, xylanase or a mixture of TLXI and xylanase) were incubated during 30 min at room temperature and pH 5.0 (25 mM sodium acetate buffer). The gels were silver stained in accordance with GE Healthcare development technique file 210.

Results and discussion

Structural features of TLXI

The 3D structural model of TLXI [23] shows that it consists of mainly of β-strands and that the α-helices, present in the thaumatin structure [26], are absent in TLXI (Figure 1). The alignment of the amino acid sequence of TLXI with that of thaumatin shows a deletion of 50 amino acids (Figure 2), corresponding to domain II of thaumatin which contains the α-helices. Thus, like other short-chain TLPs with a M_r between 15,000 and 19,000, TLXI lacks this domain.

The TLXI structure shows a total of 12 β-strands organised in 3 β-sheets. The main body of the structure consists of 2 β-sheets, forming a β-sandwich. Both sheets exhibit a right-handed twist and the β-strands of one sheet are almost parallel to and on top of those of the other sheet. Each of the 12 β-strands is antiparallel to its neighbours with the exception of the N- and C-terminal strands, which are parallel to each other.

The circular dichroism (CD) spectrum of TLXI (Figure 3) confirmed the absence of α-helices in the TLXI structure, much as noted earlier [23] for its recombinant counterpart as the characteristic dual minimum at 208 and 222 nm for α-helices was not seen. The spectrum shows a single minimum between 210 and 215 nm and an increase at 200 nm, typical for antiparallel β-sheets.

The 3D structure shows five disulfide bridges. In order to verify whether all ten cysteine residues are indeed engaged in disulfide bridges, the number of free cysteine residues in a reduced TLXI sample was compared to that in an untreated sample. Table I shows that TLXI in its native form contains no free cysteine residues and that reduction with sodium borohydride results in ten cysteine residues per molecule, proving that all cysteines are involved in disulfide bridges. The mass spectrometry data confirm this result. Next to a peak at M_r 15,632.5, peaks corresponding to the TLXI peptide chain with different degrees of glycosylation were observed [10]. The calculated M_r of the TLXI peptide chain, based on its amino acid sequence, assuming that all cysteines occur as cystines (15,632.8), is thus in nearly perfect agreement with the M_r of the TLXI protein without glycosyl moieties.

Journal of Enzyme Inhibition and Medicinal Chemistry Downloaded from informahealthcare.com by Malmo Hogskola on 12/26/11
For personal use only.

RIGHTSLINK

Journal of Enzyme Inhibition and Medicinal Chemistry Downloaded from informahealthcare.com by Malmo Hogskola on 12/26/11
For personal use only.

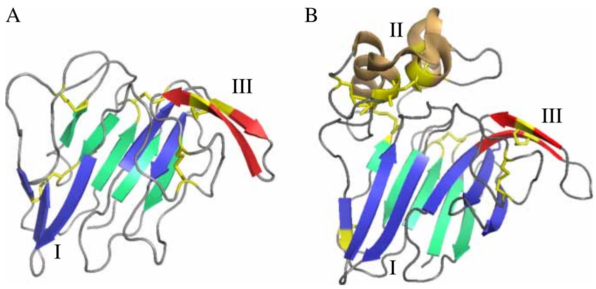

Figure 1. Comparison of the structure of TLXI (A, based on [23]) with that of thaumatin (B, based on [26]). The different domains are indicated by I, II and III. Disulfide bridges are shown in light grey. The large ß-sheets shown in light and dark grey form a ß-sandwich. A third smaller ß-sheet is shown on the right hand side of the molecules. The α-helices of thaumatin are shown as right-handed coils. The structures are visualized with Pymol 0.99rev8 [31].

Based on the structural model, the positions of the disulfide bridges were determined. They occur between cysteine residues 9 and 150, 54 and 64, 69 and 76, 115 and 138, and 123 and 128. These positions are similar to those described in other short-chain TLP models (PDB entry 2DOV, 2DOW, 2DOX, 2DOZ) [27], of which Figure 2 aligns the amino acid sequences with those of TLXI and thaumatin.

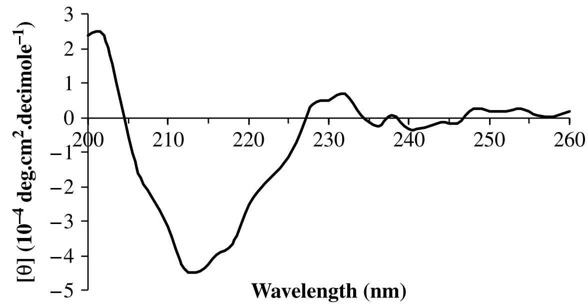

Figure 3. Circular dichroism spectrum of TLXI. The spectrum is normalized to the protein concentration and expressed as mean residue ellipticity [θ].

Stability of TLXI

Due to the presence of glycan moieties [10] and five disulfide bridges in its secondary structure, we

```
Thaumatin   --ATFEIVNRCSYTVWAAASKGDAALDAGGRQLNSGESWTINVEPGTNGGKIWARTDCYF 58
PWIR2       --ATFNIKNNCGSTIWPAGIP-----VGGGFELGAGQTSSINVPAGTKAGRIWARTGCSF 53
pPIR2       --ATFTITNRCSFTVWPAATP-----VGGGVQLSPGQTWTINVPAGTSSGRVWGRTGCSF 53
TLP1        --ATFNIKNNCGSTIWPAGIP-----VGGGFELGSGQTSSINVPAGTQAGRIWARTGCSF 53
TLP2        --ATFNIKNNCGSTIWPAGIP-----VGGGFELGSGQTSSINVPAGTQAGRIWARTGCSF 53
TLP4        --RSFSITNRCSFTVWPAATP-----VGGGRQLNGGETWNLDIPDGTSSARIWGRTDCSF 53
TLP3        TSTPLTITNRCSFTVWPAVAP-----AGLGTELHPGANWSVDESAFDSPASIWGRTGCSF 55
TLXI        --APLTITNRCHFTVWPAVALV-LHQGGGGTELHPGASWSLDTPVIGS-QYIWGRTGCSF 56
               .: * *.*  *:*.*         . * :*  * . .::     .   :*.**.* *

Thaumatin   DDSGSGICKTGDCG-GLLRCKR-FGRPPTTLAEFSLNQYG-KDYIDIS-NIKGFNVPMNF 114
PWIR2       NGGS-GSCRTGDCG-GQLSCSL-SGRPPATLAEYTIGGGGTQDFYDIS-VIDGFNLAMDF 109
pPIR2       DGSGRGSCATGDCA-GALSCTL-SGQKPLTLAEFTIGGS--QDFYDLS-VIDGYNVAMSF 108
TLP1        NGGS-GSCQTGDCG-GQLSCSL-SGQPPATLAEFTIGGGSTQDFYDIS-VIDGFNLAMDF 109
TLP2        NGGS-GSCQTGDCG-GQLSCSL-SGRPPATLAEFTIGGGSTQDFYDIS-VIDGFNLAMDF 109
TLP4        NGNS-GRCGTGDCG-GALSCTL-SGQPPLTLAEFTLGGG--TDFYDIS-VIDGYNLPMDF 107
TLP3        DAAGSGLCRTADCG-SGLRCATTDPPAPVTRAQVASSEG--FYHYGIT-TDKGFNLPLDL 111
TLXI        DRAGKGRCQTGDCGGSSLTCGG-NPAVPVTMAEVSVLQG--NYTYGVTSTLKGFNLPMDL 113
            :  . * * *.**. . * *       * * *: :          .::   .*:*:.:.:

Thaumatin   SPTTRGCRGVRCAADIVGQCPAKLKAPGGGCNDACTVFQTSEYCCTTGKCGPTEYSRFFK 174
PWIR2       S----------CSTGDALQCRD-------------------------------------- 121
pPIR2       S----------CSSGVTVTCRD-------------------------------------- 120
TLP1        S----------CSTGDALQCRD-------------------------------------- 121
TLP2        S----------CSTGDALQCRD-------------------------------------- 121
TLP4        S----------CSTGVNIQCRD-------------------------------------- 119
TLP3        T----------CSSGDALRCRE-------------------------------------- 123
TLXI        K----------CSSGDALPCRK-------------------------------------- 125
            .          *::.    *

Thaumatin   RLCP--DAFSYVLDKPTTVTCPGSSNYRVTFCPTA 207
PWIR2       PSCPPPQAYQHPND-QATHACSGNNNYQITFCP-- 153
pPIR2       SRCP--DAYLFPEDNTKTHACSGNSNYQVVFCP-- 151
TLP1        PSCPPPQAYQHPND-VATHACSGNNNYQITFCP-- 153
TLP2        PSCPPPQAYQHPND-VATHACSGNNNYQITFCP-- 153
TLP4        RNCP--DAYHTPPE-PKTKACSGNRRFNIVFCP-- 149
TLP3        EGCH--DAFPYVEFNEHACTAAG-SRLQIVFCP-- 153
TLXI        AGCD--VVQPYAKS----CSAAG-SRLQIVFCP-- 151
              *    .           :..*  . .:.***
```

Figure 2. Sequence alignment (ClustalW) of short TLPs from barley (TLP 1, 2, 3, 4) [27], wheat (PWIR2) [32] and rice (pPIR2) [33], thaumatin [34] and TLXI. Domain III is indicated with a grey arrow, while domain II is indicated with a black arrow. The rest of the protein constitutes domain I. The conserved cysteine residues are indicated in bold and the symbols above indicate which residues form disulfide bonds.

Table I. Analysis of the number of free cysteine residues in one TLXI molecule, determined with Ellmann's reagent. The number found in a TLXI sample treated with sodium borohydride was compared with the number in an untreated TLXI sample.

	Reduced		Non-reduced
Amount of TLXI (nmol)	0.6	1.3	3.2
Amount of free cysteine residues (nmol)	6.6	12.9	0.1
Number of free cysteine residues per molecule	10.2	10.1	0.0

expected TLXI, like other TLPs, to have high pH and temperature stabilities. Under the experimental conditions, TLXI was stable between pH 1 and 12 for at least 120 min (Figure 4A). A drastic decrease in inhibition activity was observed only at pH 13. At pH 5.0, TLXI was stable for at least 40 minutes at all tested temperatures (40°C–80°C) (Figure 4B). Moreover, even after 120 minutes at 100°C no decrease in inhibition activity could be observed (Figure 4C).

The resistance to proteolytic attack of TLXI was compared to that of the reference protein BSA. BSA was used as a reference protein because its percentage of disulfide bridges is comparable to that in TLXI. While BSA was completely degraded after 30 min incubation with pepsin (Figure 5, lane 2), for TLXI only a decrease in concentration could be observed (Figure 5, lane 4). Degradation products were observed in both samples after incubation with pepsin. They probably not only originate from BSA and TLXI, but also from pepsin (no pepsin band of 34,500 is seen). These results demonstrate that TLXI is more resistant to proteolytic degradation than the reference protein BSA.

TLPs are, in general, believed to be very stable under harsh conditions due to the intramolecular disulfide bridges. This is clearly also the case for TLXI, which, in contrast to TAXI and XIP, withstands extreme pH and temperature conditions. Indeed, TAXI drastically loses activity after 120 minutes incubation at pH conditions outside the range of pH 3.0 to pH 12.0. The inhibition activity of TAXI is decreased drastically after 40 min incubation at temperatures above 70°C. TAXI is deactivated at 100°C with a half-life time between 3.5 and 4.5 minutes [28]. For XIP, limited thermal stability data are available. However, its proteinaceous nature was demonstrated based on loss of its inhibition activity after 15 minutes boiling [9]. When we determined its resistance to boiling in the same way as done for TLXI, this resulted in a half-life value of less than 30 seconds (results not shown).

In addition to its resistance to extreme pH and temperature conditions, TLXI is much more resistant to degradation by pepsin than BSA. In contrast, XIP is protease sensitive, since its inhibition activity is nullified after treatment with pronase and subtilisin [9].

Optimal working conditions of TLXI

Figure 6 shows the relative xylanase activities of XTL1, XPF, XTV and XAN as well as the relative inhibition activities of TLXI towards these enzymes under varying temperature and pH conditions.

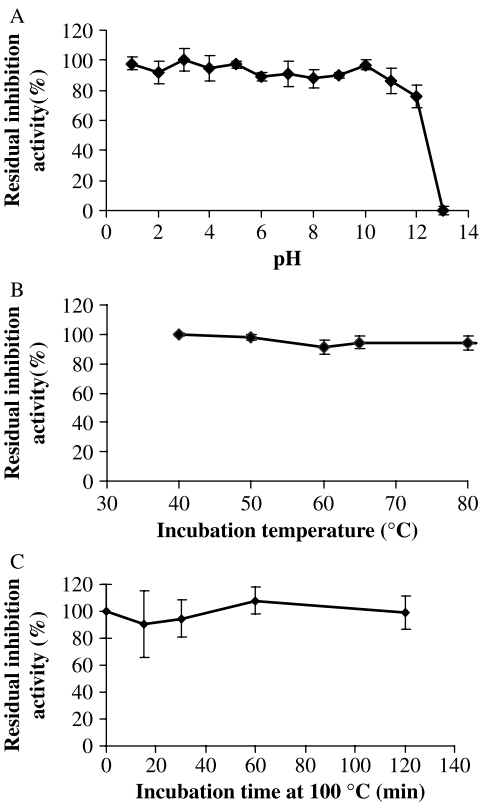

Figure 4. Residual inhibition activity of TLXI against XTL1 after 2 h incubation at different pH conditions and at room temperature (S.D. ≤ 5.7; n = 3) (A). Residual inhibition activity of TLXI against XTL1 after 40 min incubation at different temperatures and pH 5.0 (S.D. ≤ 3.9; n = 3) (B) and after different times at pH 5.0 and 100°C (S.D. ≤ 9.7; n = 3) (C).

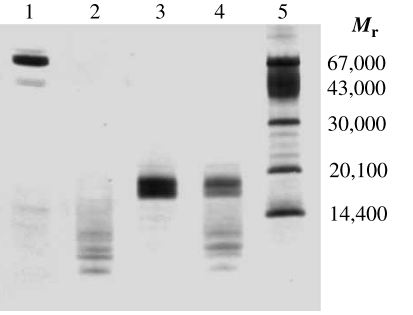

Figure 5. SDS-PAGE profile illustrating the resistance to proteolytic degradation by pepsin. TLXI samples (lanes 3 and 4) are compared with BSA samples (lanes 1 and 2) under reducing conditions, after 30 min at 37°C in the absence (lane 1 and 3) and the presence of pepsin (lane 2 and 4). The sizes of the M_r markers (lane 5) are indicated on the right. The gel was silver stained.

Journal of Enzyme Inhibition and Medicinal Chemistry Downloaded from informahealthcare.com by Malmo Hogskola on 12/26/11
For personal use only.

RIGHTSLINK

Journal of Enzyme Inhibition and Medicinal Chemistry Downloaded from informahealthcare.com by Malmo Hogskola on 12/26/11
For personal use only.

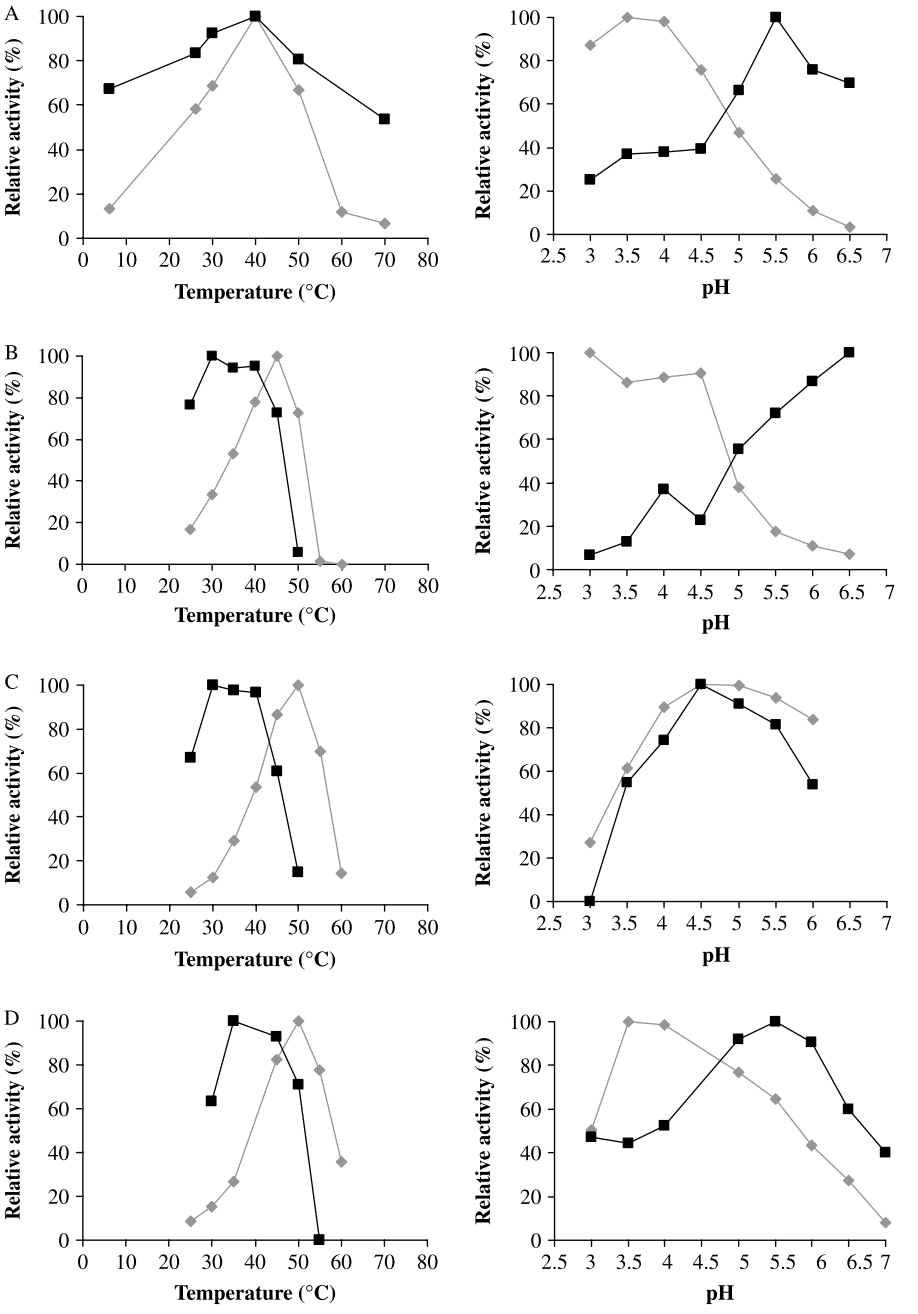

Figure 6. Relative inhibition activities of TLXI (■) against XTL1 (A), XAN (B), XTV (C) and XPF (D) and relative xylanase activities in the absence of TLXI (◆) at different temperatures (left) and pH conditions (right).

XTL1 is optimally active at 40°C. The optimal temperature for XAN is 45°C, while the activities of XTV and XPF are maximal at 50°C. The pH optima does not exceed pH 4.5 for any of the tested xylanases.

In general, the maximum inhibition activity of TLXI is recorded at temperatures between 30 and 40°C. The optimal pH conditions for inhibition of XTL1, XTV and XPF are 5.5, 4.5 and 5.5, respectively. For XAN, an increasing inhibition activity is measured starting from pH 4.5. For the determination of the optimal pH conditions for inhibition of the latter enzyme, a problem is that the optimal pH for inhibition is situated in the range where the enzyme activities are low. Under these conditions, it is difficult to obtain an accurate estimation of the optimal inhibition conditions, as the error for the determination of the inhibition activity increases with decreasing enzyme activity. Nevertheless, based on these results, pH 5.0 and 40°C are selected for measurement of inhibition activity of TLXI using the Xylazyme-AX method. At this pH, a good compromise is reached between xylanase and inhibition activities.

The optimal conditions for the inhibition of xylanases by TLXI are compared to those for TAXI and XIP. TAXI inhibits the GH11 xylanase from

RIGHTSLINK

Journal of Enzyme Inhibition and Medicinal Chemistry Downloaded from informahealthcare.com by Malmo Hogskola on 12/26/11
For personal use only.

Bacillus subtilis (XBS) and XAN optimally at pH 5.0. The optimal temperature for inhibition of XAN by TAXI is 40°C. However, for XBS inhibition by TAXI, a lower optimal temperature was noted, *i.e.* 20 to 30°C [28]. Much as noted for TLXI here, the inhibition activity of XIP towards XAN increases between pH 4.5 and 6.5 [14]. The optimal temperature for inhibition by XIP of XAO and XTL2 are 30°C (results not shown). Therefore, for the enzymes tested, the optimal temperature for inhibition by XIP is lower than that for inhibition by TLXI.

Because of the limitations of the Xylazyme-AX method for measuring the inhibition activity in the pH ranges where the xylanase activity is low, isoelectric focusing titration curve (IEFTC) analysis was used to study the pH-dependencies of the interaction between TLXI on the one hand, and XTL1 and XAN on the other hand (Figure 7). The obtained result confirmed the previously determined pI value of TLXI [10]. Figure 7 III shows the migration pattern of TLXI in a gel with a pH 3.0 to 9.0 gradient. While at pH 3.0 TLXI migrates completely towards the negatively charged cathode, at pH 9.0 no mobility is seen, indicating that TLXI is uncharged. The pI value of TLXI is thus approximately 9.0, while those of XTL1 and XAN are around 5.5 and 3.0, respectively (Figure 7 I).

The absence of complex dissociation on IEFTC gels demonstrated that the complex formed between TLXI and XTL1 is stable in the pH range 3.0 to 9.0 (Figure 7A II). This is in line with the results in Figure 6A, i.e. that TLXI exhibits inhibition activity towards XTL1 over the whole pH 3.0 to pH 6.5 range.

The IEFTC gels shows that the XAN-TLXI complex is stable at least between pH 4.0 and 7.5 (Figure 7B II). Outside this range, neither complex, nor free enzyme or inhibitor are seen. Therefore, no conclusion can be drawn for the more extreme pH conditions. This is in line with the results of Figure 6B, which also shows that TLXI inhibits XAN in the pH 4.0 to pH 6.5 range. In the lower part of the tested pH-range (pH 3.0 to 3.5), the inhibition activity is limited. In the upper part of the tested pH-range (pH 6.0 to 6.5), the xylanase activity is too low to accurately determine the inhibition activity, much as seen for XTL1 in Figure 6A.

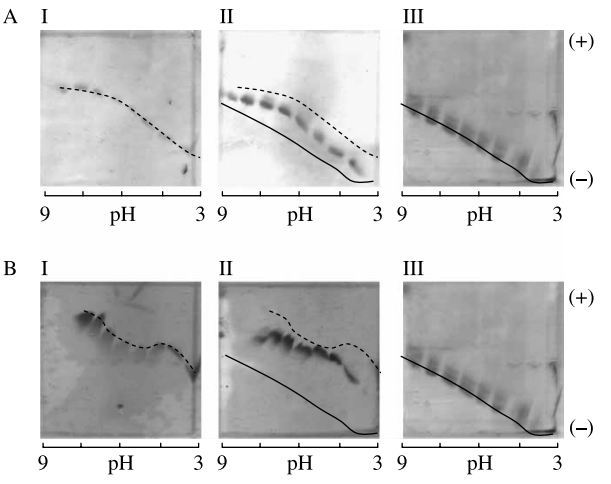

Figure 7. Iso-electric focusing titration curves showing the interaction between TLXI and XTL1 (A) and XAN (B). For each xylanase, a gel is shown with the xylanase (I), the mixture of xylanase and TLXI (II) and TLXI (III). The samples were incubated during 30 min at room temperature and pH 5.0 (25 mM sodium acetate buffer) prior to application on the gels. The cathode and anode are indicated by (−) and (+), respectively.

Similar experiments earlier showed that the complex between TAXI and XAN is stable over a narrower pH range (pH 3.0 to 7.0) than the TAXI-XTL1 [29] and TAXI-XBS complexes [30] which occur over the whole pH range of the IEFTC gel, *i.e.* pH 3.0 to 9.0. XIP-XAN complex was detected between pH 4.0 and 7.5. It is thus considerably less stable than the complex of XIP with a GH10 xylanase from *A. nidulans* which was observed between pH 3.0 and 9.0 [14].

Conclusion

In conclusion, TLXI is a very stable protein. It is stable for at least 120 minutes between pH 1–12 and for at least 120 minutes at 100°C. This high stability is probably due to the presence of a high number of disulfide bridges, much as seen for other thaumatin-like proteins. Five disulfide bridges and only β-sheets are seen in the TLXI structural model and these structural features are experimentally verified. Much as in the structures of other short-chain thaumatin-like proteins, no α-helix is present.

TLXI has optimal working conditions comparable to those of the two earlier described xylanase inhibitors from wheat, TAXI and XIP. Its inhibition activity shows a maximum at approximately 40°C and pH 5.0.

Acknowledgements

The authors wish to acknowledge 'Instituut voor de aanmoediging van Innovatie door wetenschap en technologie' in Vlaanderen (IWT, Brussels, Belgium) for financial support. Kurt Gebruers is a postdoctoral fellow of the 'Fonds voor Wetenschappelijk Onderzoek-Vlaanderen' (FWO-Vlaanderen, Brussels, Belgium). This study was in part carried out in framework of research project GOA/03/10 financed by the Research Fund K. U. Leuven. We thank Prof. Paul Proost for the help with the MS analysis.

Declaration of interest: The authors report no conflicts of interest. The authors alone are responsible for the content and writing of the paper.

References

[1] Dekker RFH, Richards GN. Hemicellulases: their occurrence, purification, properties, and mode of action. Adv Carbohydr Chem Biochem 1976;32:277–352.

RIGHTSLINK

Journal of Enzyme Inhibition and Medicinal Chemistry Downloaded from informahealthcare.com by Malmo Hogskola on 12/26/11
For personal use only.

[2] Courtin CM, Delcour JA. Arabinoxylans and endoxylanases in wheat flour bread-making. J Cereal Sci 2002;35:225–243.
[3] Debyser W, Derdelinckx G, Delcour JA. Arabinoxylan solubilisation and inhibition of the barley malt xylanolytic system by wheat during brewing with wheat whole meal adjunct: Evidence for a new class of enzyme inhibitors. J Am Soc Brew Chem 1997;55:153–156.
[4] Bedford MR. Exogenous enzymes in monogastric nutrition - their current value and future benefits. Anim Feed Sci Technol 2000;86:1–13.
[5] Christophersen C, Andersen E, Jakobsen TS, Wagner P. Xylanases in wheat separation. Starch 1997;49:5–12.
[6] Frederix SA, Courtin CM, Delcour JA. Impact of xylanases with different substrate selectivity on gluten-starch separation of wheat flour. J Agric Food Chem 2003;51:7338–7345.
[7] Coutinho PM, Henrissat B. 1999., Carbohydrate-active enzymes server at URL: http://afmbs.cnbrs-mrs/~cazy/CAZY/index.html. [cited]
[8] Debyser W, Peumans WJ, Van Damme EJM, Delcour JA. *Triticum aestivum* xylanase inhibitor (TAXI), a new class of enzyme inhibitor affecting breadmaking performance. J Cereal Sci 1999;30:39–43.
[9] McLauchlan WR, Garcia-Conesa MT, Williamson G, Roza M, Ravestein P, Maat J. A novel class of protein from wheat which inhibits xylanases. Biochem J 1999;338:441–446.
[10] Fierens E, Rombouts S, Gebruers K, Goesaert H, Brijs K, Beaugrand J, Volckaert G, Van Campenhout S, Proost P, Courtin CM, Delcour JA. TLXI, a novel type of xylanase inhibitor from wheat (*Triticum aestivum*) belonging to the thaumatin family. Biochem J 2007;403:583–591.
[11] Sansen S, De Ranter CJ, Gebruers K, Brijs K, Courtin CM, Delcour JA, Rabijns A. Structural basis for inhibition of *Aspergillus niger* xylanase by *Triticum aestivum* xylanase inhibitor-I. J Biol Chem 2004;279:36022–36028.
[12] Payan F, Flatman R, Porciero S, Williamson G, Juge N, Roussel A. Structural analysis of xylanase inhibitor protein I (XIP-I), a proteinaceous xylanase inhibitor from wheat (*Triticum aestivum*, var. Soisson). Biochem J 2003;372:399–405.
[13] Juge N, Payan F, Williamson G. XIP-I, a xylanase inhibitor protein from wheat: a novel protein function. Biochim Biophys Acta 2004;1696:203–211.
[14] Flatman R, McLauchlan WR, Juge N, Furniss CSM, Berrin JG, Hughes RK, Manzanares P, Ladbury JE, O'Brien R, Williamson G. Interactions defining the specificity between fungal xylanases and the xylanase-inhibiting protein XIP-I from wheat. Biochem J 2002;365:773–781.
[15] Beliën T, Van Campenhout S, Van Acker M, Volckaert G. Cloning and characterization of two endoxylanases from the cereal phytopathogen *Fusarium graminearum* and their inhibition profile against endoxylanase inhibitors from wheat. Biochem Biophys Res Commun 2005;327:407–414.
[16] Payan F, Leone P, Porciero S, Furniss CSM, Tahir T, Williamson G, Durand A, Manzanares P, Gilbert HJ, Juge N, Roussel A. The dual nature of the wheat xylanase protein inhibitor XIP-I—structural basis for the inhibition of family 10 and family 11 xylanases. J Biol Chem 2004;279:36029–36037.
[17] Bellincampi D, Camardella L, Delcour JA, Desseaux V, D'Ovidio R, Durand A, Elliot G, Gebruers K, Giovane A, Juge N, Soerensen JF, Svensson B, Vairo D. Potential physiological role of plant glycosidase inhibitors. Biochim Biophys Acta 2004;1696:265–274.
[18] Brutus A, Reca IB, Herga S, Mattei B, Puigserver A, Chaix JC, Juge N, Bellincampi D, Giardina T. A family 11 xylanase from the pathogen *Botrytis cinerea* is inhibited by plant endoxylanase inhibitors XIP-I and TAXI-I. Biochem Biophys Res Commun 2005;337:160–166.
[19] Igawa T, Ochiai-Fukuda T, Takahashi-Ando N, Ohsato S, Shibata T, Yamaguchi I, Kimura M. New TAXI-type xylanase inhibitor genes are inducible by pathogens and wounding in hexaploid wheat. Plant Cell Physiol 2004;45:1347–1360.
[20] Igawa T, Tokai T, Kudo T, Yamaguchi I, Kimura M. A wheat xylanase inhibitor gene, *Xip-I*, but not *Taxi-I*, is significantly induced by biotic and abiotic signals that trigger plant defense. Biosci Biotechnol Biochem 2005;69:1058–1063.
[21] Gebruers K, Debyser W, Goesaert H, Proost P, Van Damme J, Delcour JA. *Triticum aestivum* L. endoxylanase inhibitor (TAXI) consists of two inhibitors, TAXI I and TAXI II, with different specificities. Biochem J 2001;353:239–244.
[22] Brito N, Espino JJ, Gonzalez C. The endo-beta-1,4-xylanase xyn11A is required for virulence in Botrytis cinerea. Mol Plant-Microbe Interact 2006;19:25–32.
[23] Rombouts S, Fierens E, Vandermarliere E, Voet ARD, Gebruers K, Beaugrand J, Courtin CM, Delcour JA, De Maeyer M, Rabijns A, Van Campenhout S, Volckaert G. His22 of TLXI plays a critical role in the inhibition of glycoside hydrolase family 11 xylanases. J Enzym Inhib Med Ch, available online: DOI 10.1080/14756360701841913.
[24] Bradford MM. Rapid and sensitive method for quantitation of microgram quantities of protein utilizing principle of protein-dye binding. Anal Biochem 1976;72:248–254.
[25] Gasteiger E, Hoogland C, Gattiker A, Duvaud S, Wilkins MR, Appel RD, Bairoch A. Protein identification and analysis tools on the ExPASy server. In: Walker JM, editor. The Proteomics Protocols Handbook. Totowa, USA: Humana Press; 2005. p 571–607.
[26] Devos AM, Hatada M, Vanderwel H, Krabbendam H, Peerdeman AF, Kim SH. 3-Dimensional structure of thaumatin-I, an intensely sweet protein. Proc Natl Acad Sci U S A 1985;82:1406–1409.
[27] Reiss E, Schlesier B, Brandt W. cDNA sequences, MALDI-TOF analyses, and molecular modelling of barley PR-5 proteins. Phytochemistry 2006;67:1856–1864.
[28] Gebruers K, Brijs K, Courtin CM, Fierens K, Goesaert H, Rabijns A, Raedschelders G, Robben J, Sansen S, Soerensen JF, Van Campenhout S, Delcour JA. Properties of TAXI-type endoxylanase inhibitors. Biochim Biophys Acta 2004;1696:213–221.
[29] Fierens K, Gils A, Sansen S, Brijs K, Courtin CM, Declerck PJ, De Ranter CJ, Gebruers K, Rabijns A, Robben J, Van Campenhout S, Volckaert G, Delcour JA. His374 of wheat endoxylanase inhibitor TAXI-I stabilizes complex formation with glycoside hydrolase family 11 endoxylanases. FEBS J 2005;272:5872–5882.
[30] Gebruers K, Goesaert H, Brijs K, Courtin CM, Delcour JA. Purification of TAXI-like endoxylanase inhibitors from wheat (*Triticum aestivum* L.) whole meal reveals a family of iso-forms. J Enz Inhib Med Ch 2002;17:61–68.
[31] DeLano WL. The PyMOL Molecular Graphics System 2002., [cited; Available from: http://www.pymol.org]
[32] Rebmann G, Mauch F, Dudler R. Sequence of a wheat cDNA-encoding a pathogen-induced thaumatin-like protein. Plant Mol Biol 1991;17:283–285.
[33] Reimmann C, Dudler R. cDNA cloning and sequence-analysis of a pathogen-induced thaumatin-like protein from rice (*Oryza sativa*). Plant Physiol 1993;101:1113–1114.
[34] Iyengar RB, Smits P, Vanderouderaa F, Vanderwel H, Vanbrouwershaven J, Ravestein P, Richters G, Vanwassenaar PD. Complete amino acid sequence of the sweet protein thaumatin-I. Eur J Biochem 1979;96:193–204.

RIGHTSLINK